considered to be stable to all the standard deprotection conditions used in phosphoramidite based DNA synthesis technology.

Conclusion

We have described the synthesis of a building block for the sequence specific introduction of the cis–syn thymine photodimer into oligonucleotides via phosphoramidite-based solid-phase DNA synthesis methodology. The convergent nature of the route to the building block will enable the preparation of isotopically labeled and structurally modified analogues of this lesion useful for a variety studies. We have also demonstrated the successful use of this building block for the incorporation of the cis–syn thymine dimer into positions 2 and 3 of tetrathymidylate. Site-specific introduction of the cis–syn thymine dimer into a virus can now be attempted by annealing and then ligating this oligonucleotide to a complimentary gapped duplex structure by methods successfully employed for other lesions.[19,20] We have also demonstrated that the cis–syn thymine dimer is stable to the standard conditions required for deprotection of all the bases. Therefore, this building block can be used for the preparation of site specific cis–syn thymine dimer containing oligonucleotides of any sequence, in amounts and purities required for detailed biophysical, enzymological, and mutagenesis studies.

Acknowledgment. This investigation was supported in part by PHS Grant no. CA40463-01, awarded by the National Cancer Institute, DHHS, and a Petroleum Research Fund no. 15790-G4, administered by the ACS. The assistance of the Washington University High Resolution NMR Service Facility, funded in part through NIH Biomedical Research Support Shared Instrument Grant 1 S10 RR02004, and a gift from the Monsanto Company is gratefully acknowledged. We thank Dennis Moore for conducting fast atom bombardment mass spectrometry and the Midwest Center for Mass Spectrometry for conducting the high resolution work.

Registry No. 1, 110270-85-4; **6** (isomer 1), 110350-81-7; **6** (isomer 2), 110311-60-9; **7**, 87367-14-4; **8** (isomer 1), 110312-28-2; **8** (isomer 2), 110312-30-6; **9**, 110312-31-7; **10**, 110270-83-2; **11**, 110270-84-3; **12** (isomer 1), 110243-20-4; **13**, 110312-32-8; **14**, 110270-86-5; **15**, 2476-57-5.

3,4-Connected Carbon Nets: Through-Space and Through-Bond Interactions in the Solid State

Kenneth M. Merz, Jr.,[†] Roald Hoffmann,*[†] and Alexandru T. Balaban[‡]

Contribution from the Department of Chemistry and Materials Science Center, Cornell University, Ithaca, New York 14853-1301, and Department of Organic Chemistry, The Polytechnic, Bucharest, Romania. *Received January 20, 1987*

Abstract: A theoretical study of a series of "honeycombed" or "layered" 3,4-connected nets is presented. The most significant feature of this series of nets is that they have infinite stacks of carbon–carbon double bonds in close contact with each other. Two of these nets have structures that not only contain stacks of 3-connected centers but also have infinite 1-dimensional polymeric units related to *cis*-polyacetylene. We employ tight-binding band structure calculations on selected examples of these nets to determine their electronic properties. The consequences of a stacked structure are analyzed by calculating the band structure of infinite layers (stacks) of ethylenes. Some of these carbon nets may be metallic. We also show that through-space and through-bond (hyperconjugative) interactions are important in the solid state, but the overall effect of these interactions varies according to the area of k-space that is being sampled.

Pursuing our continuing interest in alternative structures of diamond and graphite,[1] we decided to study a series of 3,4-connected nets. There are a number of reasons for examining these nets: first, they have an intermediate valency between graphite (3-connected) and diamond (4-connected); second, the density of the nets we will be studying here is intermediate ($\approx$3.0 g/cm^3) between that of diamond (3.51 g/cm^3) and graphite (2.27 g/cm^3);[2] and third, these nets are interesting because they have close intrastack distances (2.3 to 2.8 Å) thereby allowing for greater (especially π) band dispersions (this may make these nets metallic).

Before proceeding to a discussion of the electronic properties of these nets we would like to review briefly the current status of the allotropy of carbon.

The structurally well-characterized allotropes of carbon are restricted to only two main types: diamond (cubic and hexagonal) and graphite (hexagonal and rhombohedral).[3] In cubic (**1**) and hexagonal diamond (**2**) each carbon atom is tetrahedrally surrounded by four other carbon atoms at a distance of 1.545 Å. The structural differences between these two diamond forms can be envisioned in this way: **1** can be imagined to consist of an infinite network of adamantyl moieties, all chair cyclohexane rings, whereas in **2** there are some chair and some boat six-membered rings. Both hexagonal (**3**) and rhombohedral (**4**) graphite contain hexagonal carbon layers linked by van der Waals forces. The difference, though, between these two forms lies in the stacking of these sheets. In **3** every third layer repeats (ABAB...) with the first and second layers displaced away from each other in such a way that one-half of the atoms in each layer are above and below the center of the hexagon in the neighboring layer. **4**, on the other hand, has every fourth layer repeating to give an ABCABC... stacking pattern.

There is some evidence for other carbon allotropes.[4] The best studied of these is karbin, sometimes called chaoite.[5,6] Its structure is thought to contain carbon in alkyne or cumulene needles, **5**. Though there has been much work on karbin, our opinion is that

[†] Cornell University.
[‡] The Polytechnic.

(1) Hoffmann, R.; Hughbanks, T.; Kertesz, M.; Bird, P. H. *J. Am. Chem. Soc.* **1983**, *105*, 4831. Hoffmann, R.; Eisenstein, O.; Balaban, A. T. *Proc. Natl. Acad. Sci. U.S.A.* **1980**, *77*, 5588. Balaban, A. T.; Rentia, C. C.; Ciupitu, E. *Rev. Roum. Chim.* **1968**, *13*, 231; erratum: *Ibid.* **1968**, *13*, 1233.
(2) These are theoretical densities calculated from idealized geometries and should be considered as an upper limit to the experimental densities.
(3) Donohue, J. *The Structure of the Elements*; Wiley: New York, 1974.
(4) See the following recent review of experimental and theoretical work: Stankevich, I. V.; Nikerov, M. V.; Bochvar, D. A. *Usp. Khim.* **1984**, *53*, 1101; *Russ. Chem. Rev.* **1984**, *53*, 640.
(5) For a review on karbin see: Mel'nichenko, V. M.; Sladkov, A. M.; Nikulin, Yu. N. *Usp. Khim.* **1982**, *51*, 736; *Russ. Chem. Rev.* **1982**, *51*, 421.
(6) Whittaker, A. G. *Science* **1978**, *200*, 763.

0002-7863/87/1509-6742$01.50/0 © 1987 American Chemical Society

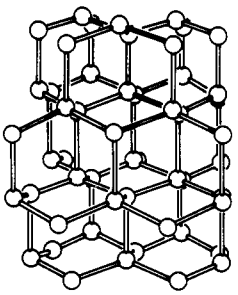

1

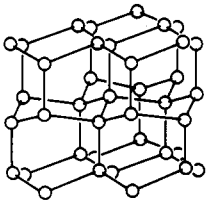

2

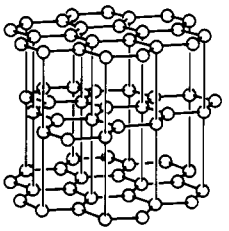

3

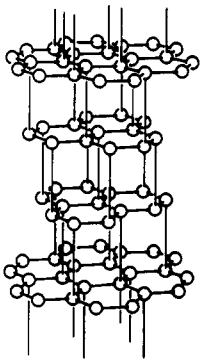

4

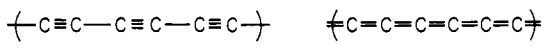

5

it remains a tantalizing mystery.

Recent NMR studies have shown that in amorphous carbon films sp^2 and sp^3 centers are present in about a 50–50% mix.[7] This implies that in amorphous carbon films regions of novel carbon allotropes, which might have conductive properties, are present. Other allotropes or phases in the carbon phase diagram have been suggested.[8] We must not pass by the seductive conjecture of a buckministerfullerene structure for C_{60}, a stable gas-phase carbon cluster.[9]

There are many theoretical studies of hypothetical carbon systems, and the reader is referred to the excellent recent review by Stankevitch, Nikerov, and Bochvar[4,10] for the appropriate references.[11]

Derivation of Stacked 3,4-Connected Nets from Plane Nets

Any enumeration of three-dimensional nets must begin with the elegant and intuitive work of Wells.[12] Wells has in fact described several 3,4-connected nets. For reasons that have to do with potential conductivity of such materials we are drawn to those nets that can be built from one-dimensional chains that are then layered or stacked by interconnecting them through their 4-connected centers. Wells has described two such nets, and we proceed to describe an outline for generating others.[12]

This is best done by example. Consider a 3-connected plane net; we choose quite arbitrarily a plane net ($(4^2.10)(4.10^2)$; **6**) that consists of four- and ten-membered rings. The notation $(4^2.10)(4.10^2)$ means that there are two inequivalent atoms, with one being part of two four- and one ten-membered ring and the other being part of one four- and two ten-membered rings. We then imagine the formation of an infinite stack of these plane nets to form a graphite like structure (**6** → **7**). The next step involves the lowering (or raising) of the shaded atoms to form 4-connected centers (sp^3 hybridized atoms) with the plane net above (below) supplying the other atoms to satisfy the valency of 4-connected carbon (**6** → **7** → **8**). Please note that this system has infinite

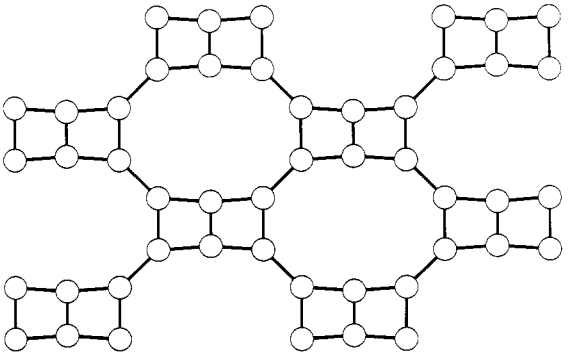

6

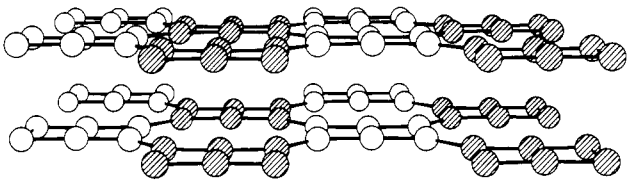

7

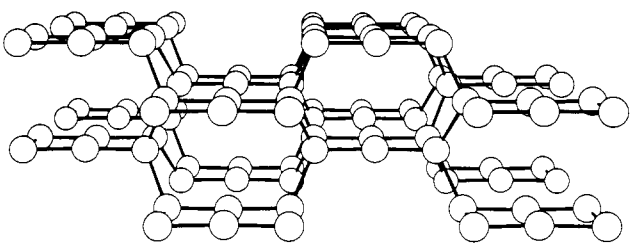

8

SPACE GROUP Immm

stacks of carbon–carbon double bonds, the interior bonds shared by two squares, which will determine the conducting (or insulating) properties of the nets. Figure 1 presents some other three-dimensional (3-D) nets and the corresponding two-dimensional (2-D) plane nets from which they were derived, in addition to **6**–**8**.

A large number of 3,4-connected nets can be derived in this manner with the number of possibilities increasing with the number of faces in the 2-D plane net (e.g., **8** has two faces while **13** has three); however, we have chosen to describe a small subset which satisfy our immediate needs. These needs are the following: the nets must be layered, they must conform to the normal valencies of carbon, and they must contain 4-connected centers that are bound to two 3- and two 4-connected centers (see **17**).

17

The structures then contain infinite polyethylene chains; more

(7) Jarman, R. H.; Ray, G. J.; Standley, R. W.; Zajac, G. W. *App. Phys. Lett.* **1986**, *49*, 1065.

(8) Matyushenko, N. N.; Strel'nitskii, V. E.; Gusev, V. A. Pis'ma *Zh. Eksp. Teor. Fiz.* **1979**, *30*, 218. Aust, R. B.; Drickamer, H. G. *Science* **1963**, *140*, 817. Bundy, F. P. *J. Chem. Phys.* **1963**, *38*, 631; *J. Geophys. Res.* **1980**, *85*, 6930.

(9) Kroto, H. W.; Heath, J. R.; O'Brian, S. C.; Curl, R. F.; Smalley, R. E. *Nature (London)* **1985**, *318*, 162.

(10) See also: Burdett, J. K.; Lee, S. *J. Am. Chem. Soc.* **1985**, *107*, 3050, 3063, 3083.

(11) This review (ref 4) was written before the C_{60} story. Opening almost any issue of a recent journal will lead to a leading reference, one of a flood, on the theory of this cluster.

(12) Wells, A. F. *Three Dimensional Nets* and *Polyhedra*; Wiley: New York, 1977. Wells, A. F. *Further Studies of Three-Dimensional Nets*; ACA Monograph No. 8, 1979.

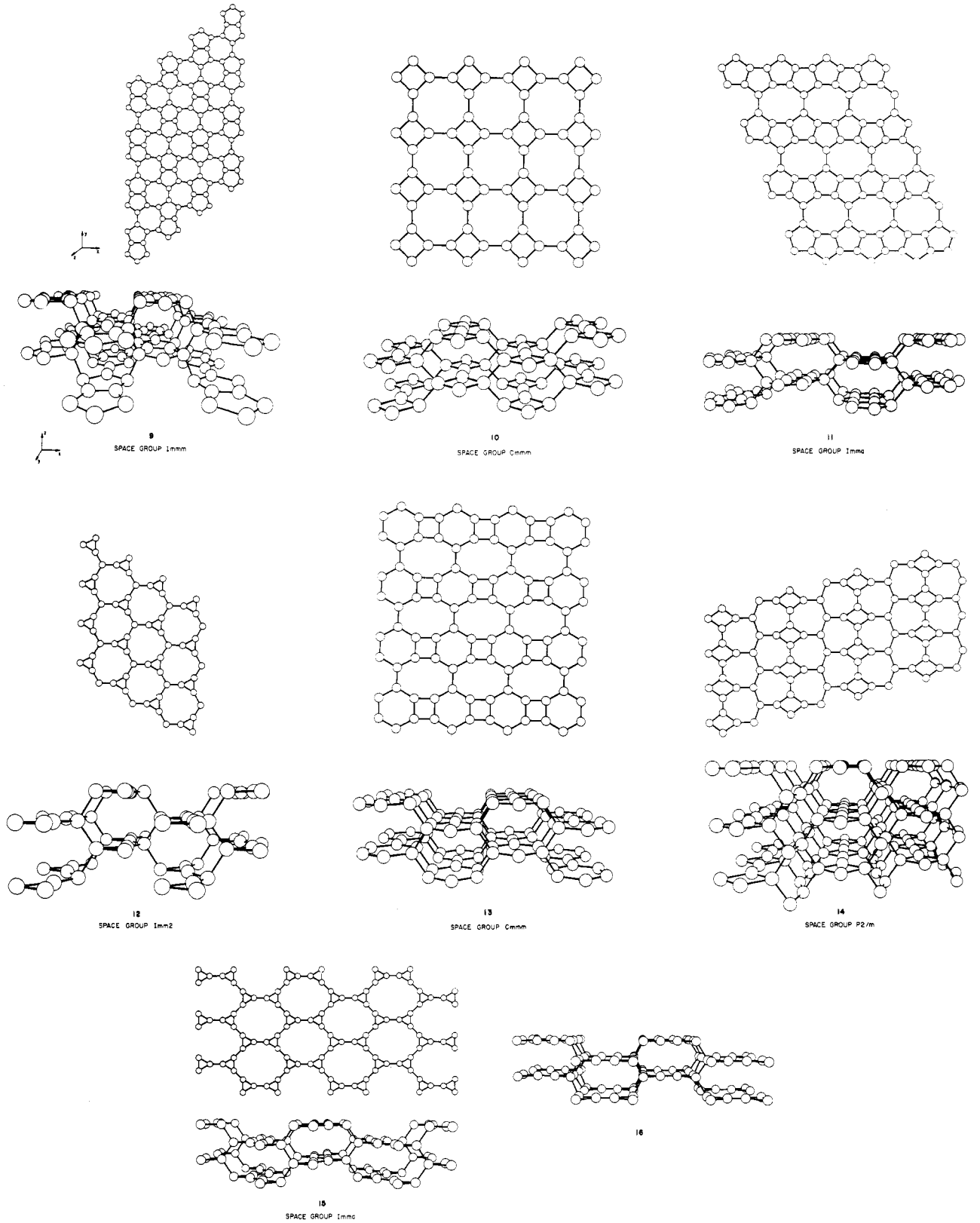

Figure 1. Further examples of layered 3,4-connected nets.

important the geometrical constraints we impose lead to stacked ethylene configurations. Last but not least the structures should be chemically reasonable.

In this paper we will be concentrating on three nets (**9**, **10**, and **11**) that we feel are representative of the nets derived above. A characteristic feature of the first two of these nets is a vertical stack of isolated carbon–carbon double bonds. Let us look at the electronic structure of a model for this structural entity.

The Band Structure of a Simple Ethylene Stack

The model we consider is **18**, a one-dimensional C_2H_4 stack. The orbitals of the monomer are well-known.[13] They are shown

(13) Jorgenson, W. L.; Salem, L. *The Organic Chemists Book of Orbitals*; Academic Press: New York 1973. Gimarc, B. M. *Molecular Structure and Bonding; The Qualitative Molecular Orbital Approach*; Academic Press: New York, 1979.

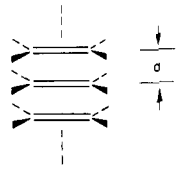

18

at the left of Figure 2. The crystal orbitals $\psi_j(k)$ are constructed by the Bloch functions where χ_l^j is the appropriate jth MO of the

$$\psi_j(k) = \sum_{l=1}^{N} e^{ikR_l}\chi_l^j$$

monomer in the l-th unit cell.[14] The center of the Brillouin zone, Γ, corresponds to $k = 0$. The zone edge, X, has $k = \pi/a$, where a is the stack spacing. At these special points the symmetry-adapted combinations are

$$\psi_j(0) = \chi^j{}_0 + \chi^j{}_1 + \chi^j{}_2 + \chi^j{}_3 + \ldots$$

(i.e., all monomer wave-functions enter with the same sign) and

$$\psi_j(\pi/a) = \chi^j{}_0 - \chi^j{}_1 + \chi^j{}_2 - \chi^j{}_3 + \ldots$$

(i.e., all monomer combinations enter with opposite sign). The consequences of this are best seen by taking the specific example of the π and π^* bands, **19** and **20**. It is clear that the $k = 0$ crystal orbitals are at high energy for both π and π^*, the $k = \pi/a$ combination lower. The band falls as one moves from the center of the zone to its edge.

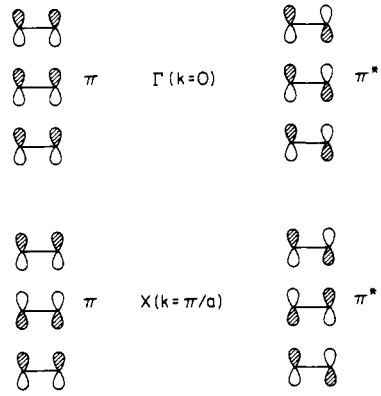

19 20

This behavior of the energy with k is, of course, a consequence of the topology of the orbitals interacting. If we examine a σ type orbital, e.g., $1a_1$ of ethylene, its energy would be expected to change with k in just the opposite way: **21** shows that the crystal orbital at Γ is more bonding than at X. Proceeding in this way we can understand the slope of every orbital in Figure 2. This figure is a schematic one, showing the evolution of the ethylene levels in the Brillouin zone (BZ). The details of the energy positions and slopes will depend on the stacking separation a. Note that the

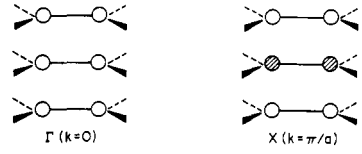

21

non-crossing rule applies to bands just as it does to individual orbitals. Since $2a_1$ and π crystal orbitals are of the same a_1 symmetry within the zone their bands do not cross. We anticipate

(14) Albright, T. A.; Burdett, J. K.; Whangbo, M.-H. *Orbital Interactions in Chemistry*; Wiley: New York, 1985.

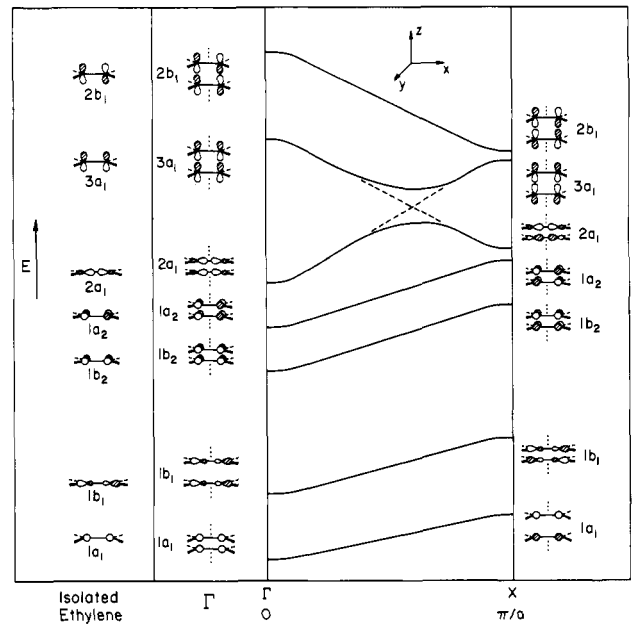

Figure 2. Qualitative band structure for **18**.

here the results of the calculations about to be described.

Now let us consider what effect the distance between the stacks might have on the band structure of this hypothetical system. As the distance decreases the band dispersion will increase the most for MOs that are pointing toward the face of an adjacent ethylene. Hence we can predict that the π bands of the stack of ethylenes should have the largest dispersion. If the dispersion increases to the point that the valence band (HOMO) overlaps with the conduction band (LUMO) we will have zero band gap (HOMO–LUMO splitting) and hence the possibility of a metallic system.

Figure 3 shows the bands of a stack of ethylenes separated by 3.0 and 2.3 Å. The van der Waals minimum for hydrocarbon π systems is around 3.3 Å so the first choice of a, the stacking separation, is in the range of moderate interaction. The value of 2.3 Å is much too close for isolated π systems. But it is what some of these 3,4-connected nets force, and so it is interesting to examine this strongly interacting model.

One way to follow the evolution of the many orbitals is simply to plot the density of states (DOS). This is the number of orbitals or levels within a given energy range. DOS plots for **18** at an inter-ethylene separation of 3.0 Å are in Figure 3a, and for 2.3 Å in Figure 3b. The π and π^* bands overlap at the shorter distance—the dispersions are so great that the bottom of the π^* band is below the top of the π band. To put it another way: At a distance of 3.0 Å the stack of ethylenes behaves as an insulator, with the band gap being significant. In this situation the π band is completely filled and the π^* is unfilled (see the shaded portions of the DOS in Figure 3a). On the other hand, if the stacks are at a distance of 2.3 Å the band gap is zero and the stack should behave as a conductor. In this case the π and π^* bands overlap and hence these bands are only partially filled (see the DOS in Figure 3b).

In the three-dimensional nets we are about to discuss, the stacking separation varies. At what point might we expect a chance of conducting behavior? Figure 4 shows the width of the π and π^* bands of a stack of ethylenes as a function of their separation, a. It is clear that the bands will begin to overlap around $a = 2.4$ Å.

Three-Dimensional Nets

All the nets we have constructed (**8**–**16**) have carbon–carbon double bonds stacked above each other. The stacking separation is set by the geometrical constraints of the lattice—one wants to keep the 4-connected center's angles close to tetrahedral and introduce as little angular strain as possible at the 3-connected

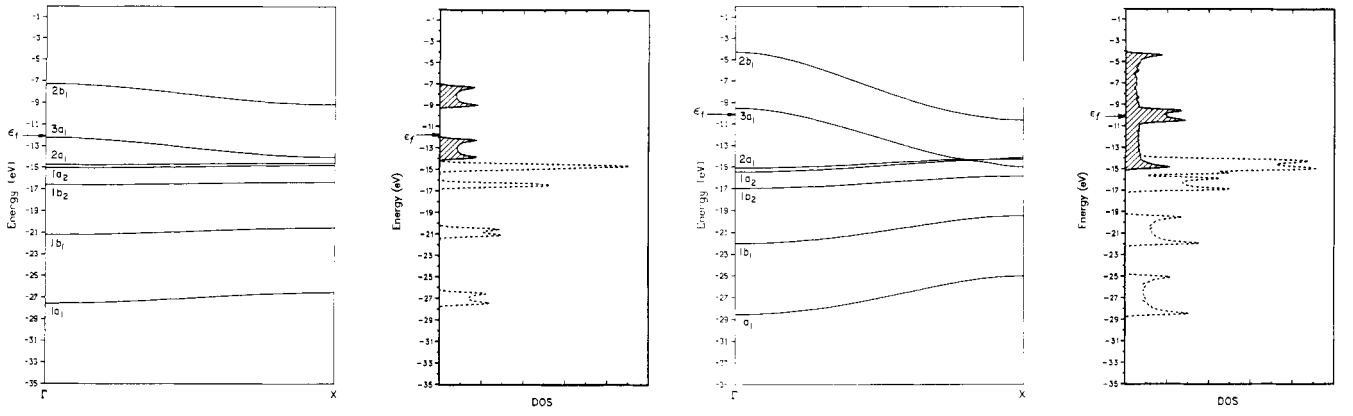

Figure 3. Calculated band structure and DOS plots for **18** at intrastack distances of (a) 3.0 Å and (b) 2.3 Å.

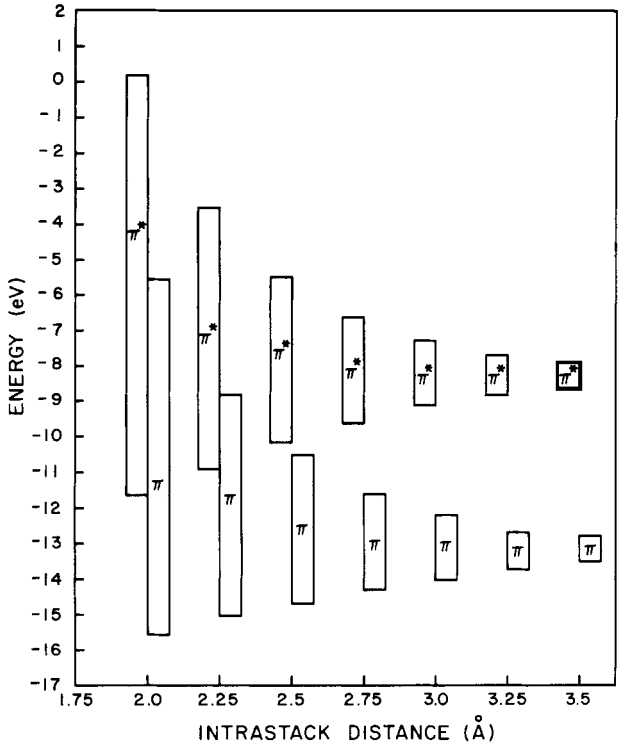

Figure 4. Effect of the intrastack separation, *a*, on the dispersion of the π and π^* bands.

carbons. We do not have a reliable structure optimization program available—if we did we could home in on the compromise between angle strain and π-system repulsion that is likely to control the geometry of these lattices. For the moment all we can do is make a reasonable guess of the geometry (see Appendix). The stacking separation that results from these geometries ranges from 2.34 to 3.0 Å. Let us discuss three systems in further detail.

The structure of **9** (see Figure 1) clearly contains one-dimensional chains of bicyclo[3.3.0]hexenes, or tetrahydropentalenes, linked up by double bonds. A model one-dimensional chain is obviously **22**, where the 4-connected centers are terminated by hydrogens. The calculated band structure and DOS for **22** are given in Figure 5.

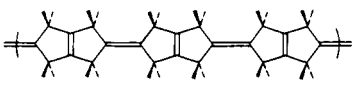

22

Chain **22** has two isolated double bonds per unit cell. We would not expect it to be a conductor by itself, and it is not. That some of the π-type bands have dispersion is due not as much to the long-distance π overlap as it is to interactions through π-type CH_2 combinations. Each CH_2 group has an appropriate σ_π (**23**) and σ_π^* (**24**) combination. These interact with the π system in a hyperconjugative or through-bond way.[15]

23, σ_π **24**, σ_π^*

The importance of these hyperconjugation effects can be seen in the DOS plots of Figure 5. Figure 5b has the π contribution of the total DOS projected out (see lined portions) while Figure 5c has the σ_π contribution projected out. By comparing these two DOS plots one notices that several of the π and σ_π resonances appear at the same location, which is indicative of the mixing of the π and σ_π type orbitals in a through-bond way.

We next build up the 3-D structure by linking these infinite 1-D polymers through their 4-connected centers; this results in **9**. The band structure for **9**, plotted along selected symmetry lines of the BZ, is presented in Figure 6. The intrastack distance that was forced by our geometrical assumptions in this case was 2.8 Å, and from our previous discussions we might expect this 3-D net to be an insulator or semiconductor. From the band structure (Figure 6) we see that this is the case because there is a significant band gap between the π and π^* levels of **9**.

We should discuss our choice of Brillouin zone. The unit cell for **9** is body-centered orthorhombic and therefore the zone used in our calculations will correspond to the body-centered orthorhombic direct lattice if one uses the primitive basis (see **25**) to generate the unit cell.[16] On the other hand a larger basis, the centered basis (see **26**), could be used and the Brillouin zone that

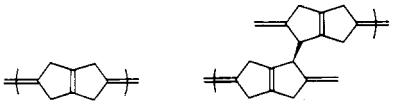

25 **26**

corresponds to this basis is the one generated from a simple orthorhombic direct lattice. We have decided to use the latter alternative even though its use results in more energy bands. The reason for the proliferation of bands is easily understood: if one increases the number of atoms in the basis the number of individual unit cell MOs increases. Each MO of the cell leads to a band. The reason why we chose to use the centered basis is because we felt that both the analysis and presentation of our results would be simplified. It should be stressed that either method of generation of the band structure will give us the same conclusions.

(15) Hoffmann, R. *Acc. Chem. Res.* **1971**, *4*, 1. Gleiter, R. *Angew. Chem., Int. Ed. Engl.* **1974**, *13*, 696. See ref 13 also.

(16) Ashcroft, N. W.; Mermin, N. D. *Solid State Physics*, Holt, Reinhart and Winston: Philadelphia, 1976.

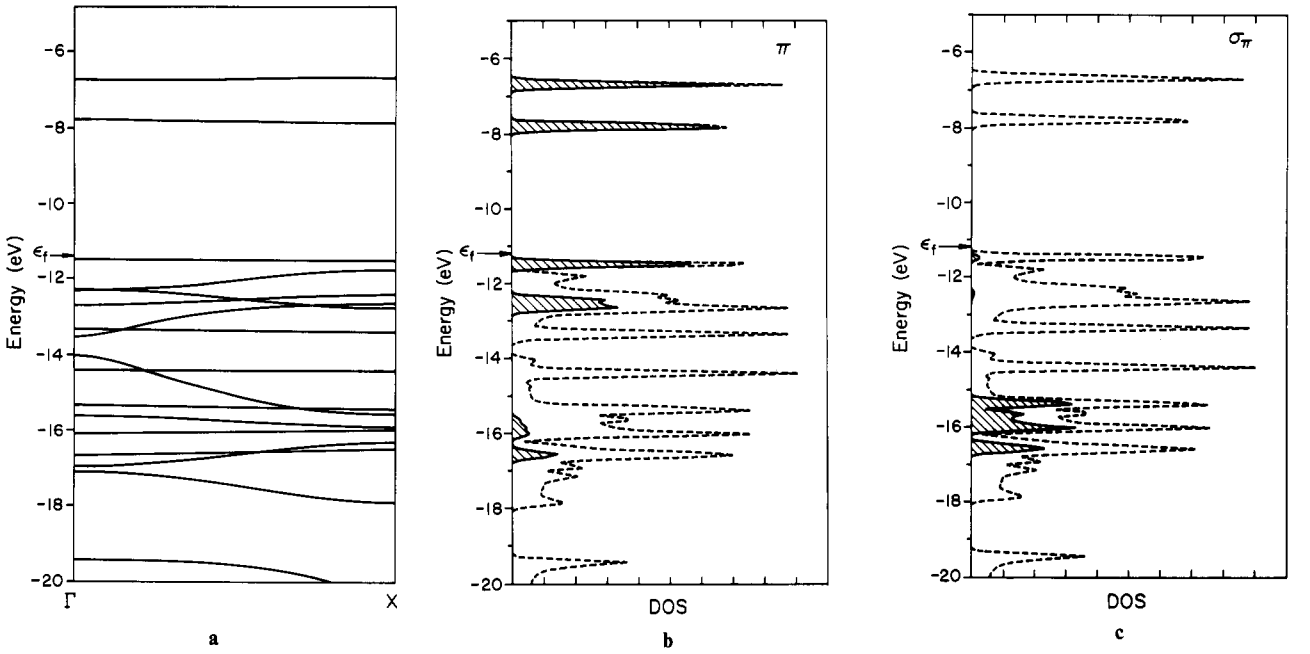

Figure 5. Calculated band structure (a) and DOS plots of π (b) and σ_π (c) type orbitals for **22**.

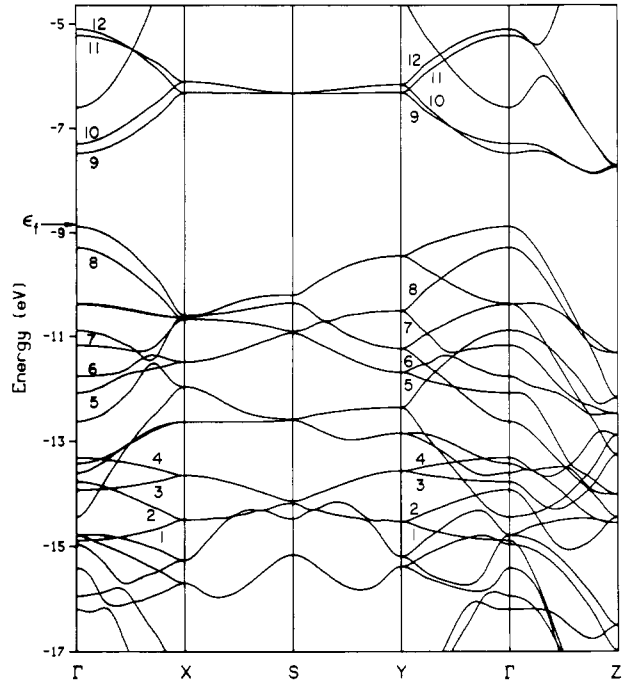

Figure 6. Calculated band structure **9**.

The band structure of **9** (Figure 6) has several features worth noting: first, the π bands along Y to Γ have been significantly spread out compared to the bands of the 1-D polymer (see Figure 5; the Y to Γ line corresponds to the axis of the 1-D polymer). The reason why this occurs is because of hyperconjugation. Recall that in the 1-D case there was significant π and σ_π mixing. This interaction affected the number of bands, but it did not influence greatly their dispersions. In the 3-D case, though, we have to remember that as we translate along Y to Γ we are creating intercell σ bonds. Since most of these π bands have σ_π mixed into them, they are therefore very sensitive to the creation of intrastack σ bonds. The σ bonding starts out being bonding (or antibonding) at the zone center, but as we proceed to the zone edge it becomes antibonding (or bonding). Hence the large band dispersions. Notice, though, some π bands remain relatively flat (e.g., 5 and 6 in Figure 6); this is because the unit cell MOs have nodes or very small coefficients at the 4-connected carbon atoms and

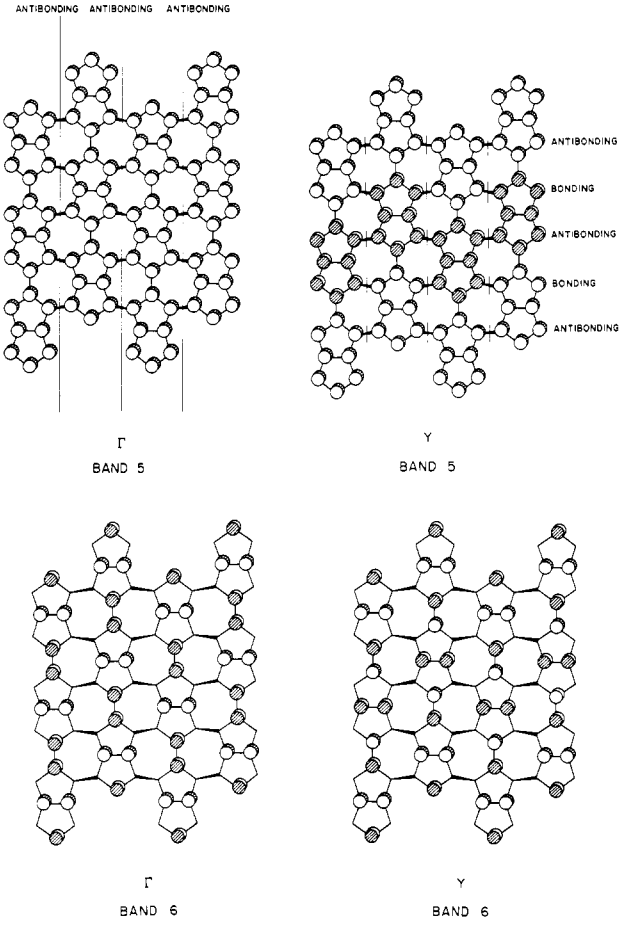

Figure 7. Variation of the orbital topologies as a function of k for **9**.

therefore these bands are insensitive to translation along Y to Γ (in terms of σ-bonding interactions; π effects remain). A qualitative picture of these interactions is given in Figure 7. The arguments presented can also be used to explain the band structure along the Γ to X line.

The greatest dispersions in Figure 6 are along the Γ–Z line. This is along the stacking direction, and the reasons for interaction are obvious. Even if 2.8 Å is not enough to produce an overlap

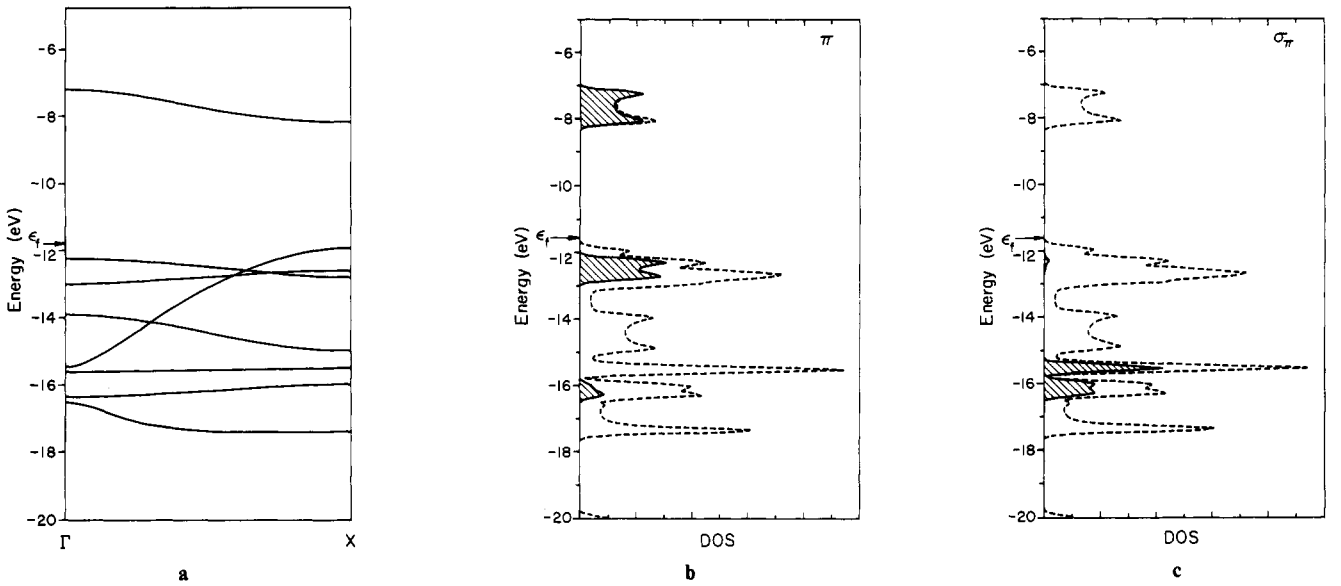

Figure 8. Calculated band structure (a) and DOS plots of π (b) and σ_π (c) type orbitals for **27**.

of π and π^* bands, it is still well below the van der Waals contact. There is substantial overlap of the p-type orbitals at this distance.

The next structure we would like to consider is **10** (see Figure 1). In this case the 3-D structure is made up of infinite 1-D chains of four-membered rings connected by double bonds. An obvious model is **27**, the band structure of which is shown in Figure 8.

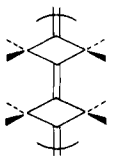

27

Hyperconjugation or through-bond coupling manifests itself clearly in this system. We can illustrate the effect by an interaction diagram (Figure 9) which focuses on one double bond and the four surrounding CH_2 units. These generate σ_π (and σ_π^*) combinations of local SS, SA, AS, and AA symmetry. Two of these symmetries match those of the π and π^* combination. It should be noted that Figure 9 is a schematic diagram, illustrating the possibilities for interaction. It is not a level picture for either **28** or **29**, though these models could also be calculated.

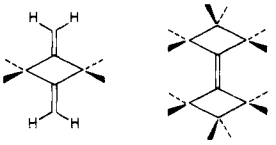

28 **29**

In the linear polymer **27** there is substantial hyperconjugation, as Figure 8 suggests. Decompositions of the DOS into CH_2 and C $2p_z$ contributions (Figure 8b,c) show the 4-connected and 3-connected carbons contribute, unequally of course, to both π and σ_π bands.

The 3-D net again can be constructed by forming bonds between the 4-connected centers in such a way as to yield **10**. The geometry we have chosen for this net gives an intrastack distance of 2.5 Å and is described in the Appendix. This net has a base-centered orthorhombic unit cell, but again we will not be using the Brillouin zone corresponding to the primitive basis, instead opting for a larger (doubled) centered basis in order to use the simple orthorhombic Brillouin zone. The band structure is given in Figure 10. This band structure suggests that **10** should be metallic because the π and π^* bands cross along the Γ to Z direction. The reason why this material is a conductor is because the π–π

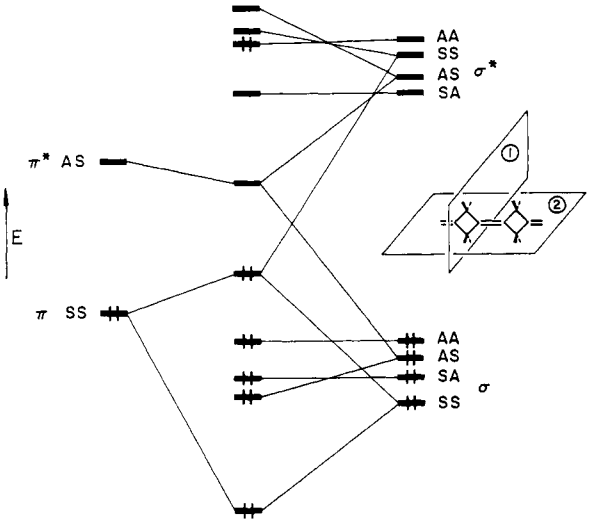

Figure 9. Qualitative interaction diagram for the π and σ_π orbitals of **27**.

through-space interaction is large enough to cause the π and π^* bands to overlap.

The band plot for **10** has one interesting feature and this is along the Γ to X line. The unit cell MOs labeled **5** and **6** are not expected to be affected by a translation along X because the p_z coefficients on the 4-connected centers are zero. Then why are these orbitals split at Γ? This has to do with the direct overlap between the p_z orbitals on the three-connected centers (atoms numbered 1 and 2 in Figure 11). This interaction is very small (the gap is only 0.05 eV), but nonetheless it does cause the observed splitting.

We next consider the structure **11** (see Figure 1). **11** can be imagined to be made up of 1-D chains of five-membered rings to give **30**. **30** is different from the previous polymeric units because this geometry allows the double bonds to be conjugated and not isolated from one another. As a result of this we have to consider several possible resonance forms; these are **31**, **32**, and **33**. **31** is the delocalized form of the localized and bond-alternating **32** and **33** and all of these can be regarded as *cis*-polyacetylene isomers with 4-connected bridges connecting the 1,4 positions together. Polymers of the polyacetylene type have been discussed by others and our group previously,[17] but we would still like to

(17) Whangbo, M.-H.; Hoffmann, R.; Woodward, R. B. *Proc. R. Soc. London, Ser. A* **1979**, *366*, 23 and references therein.

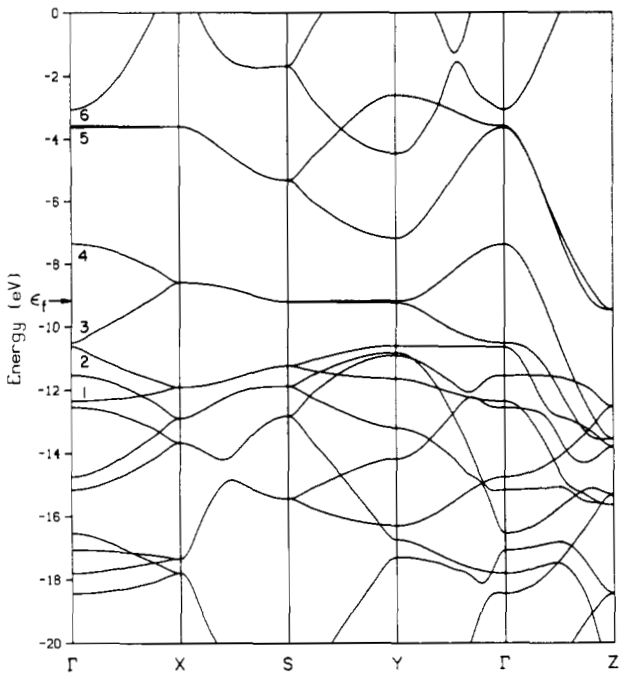

Figure 10. Calculated band structure for **10**.

examine some of the properties of these systems as they relate to the present situation. The interesting feature of the net **11** is that it has the potential of 2-D conduction: polyacetylene type π conjugation along one axis and dispersion due to the intrastack σ-type overlap of π-chains of the kind we have discussed throughout this paper along another, stacking direction

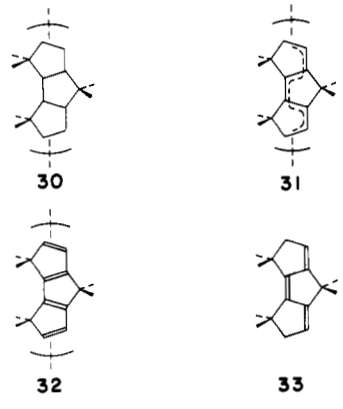

The qualitative band structure for the π bands of **30** is drawn schematically in Figure 12. There are four carbon $2p_z$ orbitals per unit cell, therefore four π bands. Degeneracies are forced by symmetry at the zone edge, but the near degeneracy of e and d (see band labels in Figure 12) at the zone center is not forced by symmetry. In fact it can be tuned by the magnitudes of various interactions. The only difference between d and e begins to be found at the level of 1,4-interactions (bonding in e, antibonding in d). These will be small, but they will produce a small splitting with e below d in **31**. Distortions to **32** or **33** will increase this splitting, in understandable ways: **33** will pull e still further down, **32** will stabilize d instead.

The calculated band structure and specific DOS plots for **31** and **33** are reproduced in parts a and b of Figure 13, respectively. The corresponding plots for **32** are similar to those of **33** and will not be given here. The π band structure for **33** is exactly what we expected, while that of **31** shows evidence of a transannular interaction because there is a small band gap and we also do observe that e is at lower energy than d. This splitting, though, is very small (0.04 eV).

Whenever a small energy gap like this is encountered one immediately thinks of a system that should be unstable to a

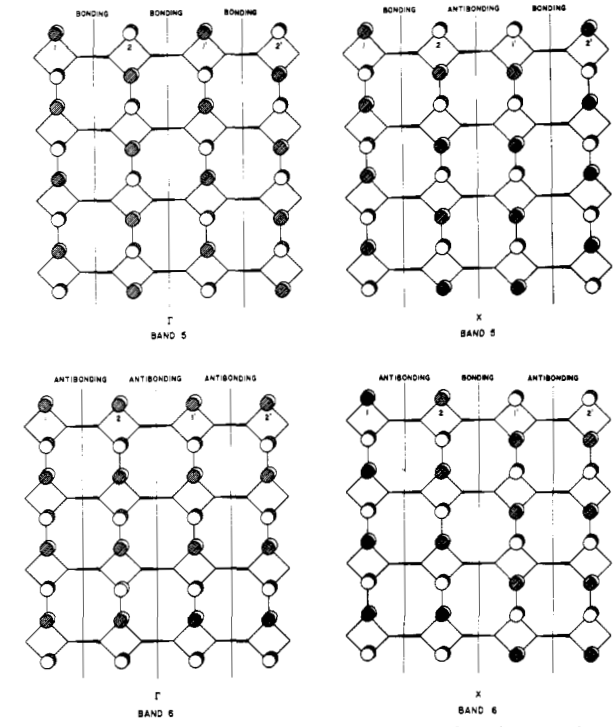

Figure 11. Variation of the orbital topologies as a function of k for **10**.

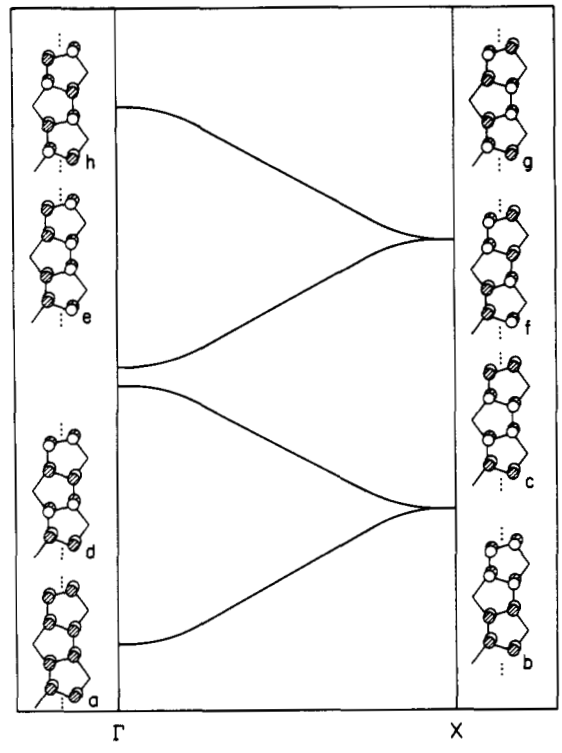

Figure 12. Qualitative π band structure for **30**.

second-order Jahn–Teller distortion[18] or as it is known in solid-state chemistry a Peierls distortion.[19] The effect of this distortion will be to convert **31** to either **32** or **33**. In order to determine this we have calculated the energy per unit cell for these structures and we arrive at the relative energy ordering of 0.75 eV (**31**), 0.8

(18) Opik, U.; Pryce, M. H. *Proc. R. Soc. London, Ser. A* **1937**, *161*, 220. Bader, R. F. W. *Can. J. Chem.* **1962**, *40*, 1164. Pearson, R. G. *J. Am. Chem. Soc.* **1969**, *91*, 4947. Pearson, R. G. *J. Mol. Struct.: Theochem.* **1983**, *103*, 25. Pearson, R. G. *Symmetry Rules for Chemical Reactions*; Wiley: New York, 1976.

(19) Peierls, R. *Quantum Theory of Solids*; University Press: Oxford, 1955.

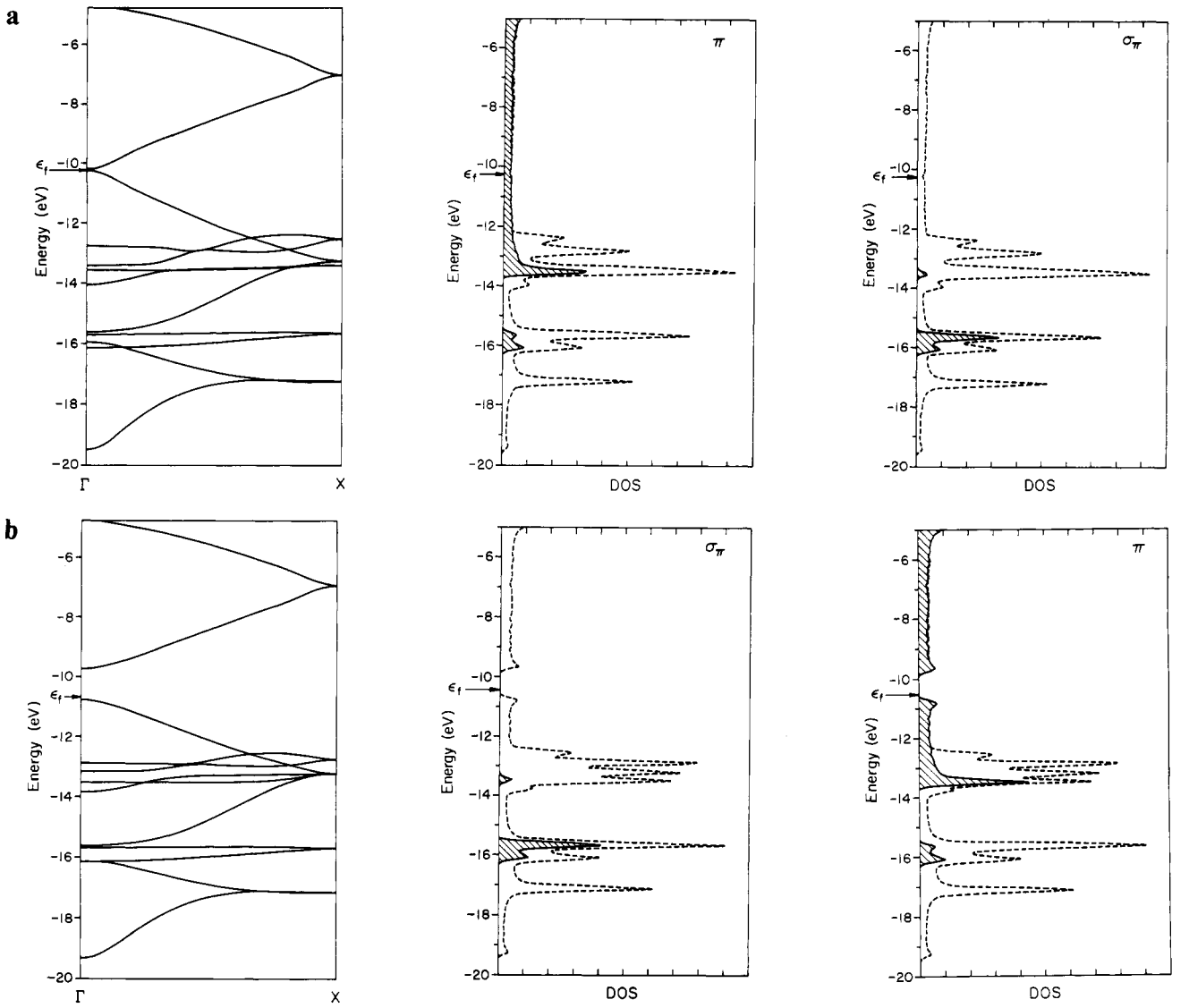

Figure 13. Calculated band structure and DOS plots of π and σ_π type orbitals for (a) **31** and (b) **33**.

eV (**32**), and 0.0 eV (**33**). While these energy trends are only approximate, it seems likely that **33** should be the most stable resonance structure.

Before continuing on to the 3-D case we should mention that we do expect this system to be affected by through-bond interactions, but since the basis we are using to generate the polymer has very low symmetry (see Figure 12) we will be unable to use it to generate the interaction diagram. However, by inspecting the DOS plots given in Figure 13, one sees that there is significant π and σ_π mixing in this polymer also.

The geometry we have chosen for **11** is such that the intrastack distance is 2.34 Å. The bond angles around the 4-connected centers are very close to what would be considered normal for a tetrahedral carbon atom (see Appendix). Because of the close intrastack contact we can immediately anticipate that **11** should be metallic (see Figure 4). Again we looked at the three possible resonance structures for **11** and they are identified as **11(31)**, **11(32)**, and **11(33)** in order to relate these 3-D structures with the previous 1-D ones. We will only reproduce the band structure for **11(33)** because the corresponding plots for **11(31)** and **11(32)** are similar and the former is the most stable of the three. The relative energy per carbon atom is 0.09 (**11(31)**), 0.11 (**11(32)**), and 0.0 eV (**11(33)**). This band structure is given in Figure 14. As in the previous two examples we have not used the primitive basis to generate the band structure, instead we have opted to use the centered basis. From the band picture for **11(33)** we see that this net should be metallic, because there is no band gap and the Fermi level crosses several bands. Now let us scrutinize the portion of this band picture that is labeled Γ–X. As before, we observe that the π bands along the Γ–X line that have σ_π character (the ones labeled 1, 2, 3, 4, 5, 6) have the largest dispersion, while the ones that have little or none have the smallest dispersion (7, 8, 9, 10). That these latter bands have any dispersion at all is entirely due to the hyperconjugative interactions between the 3-connected centers as was described in detail for **10**. Here, though, we expect this effect to cause a larger splitting (≈0.15 eV vs. 0.05 eV) because of the smaller intrastack distance.

Conclusions. We have described a series of 3,4-connected nets that have at least one structural feature in common: they all contain infinite stacks of carbon–carbon double bonds. It is this structural feature that has an overriding influence on the electronic properties of these nets. If these stacks have close intrastack contacts (<2.4 Å) the net should have metallic properties; if the contacts are longer (>2.4 Å) they will behave as insulators or semiconductors (semi-metals).

Since we have mixed valency sites in these nets (i.e. 3 and 4-connected centers) several interesting features emerge: we observe the effects of through-bond interactions which involve the mixing of π and σ_π symmetry types and there is the aforementioned strong through-space interactions between the stacks. This latter effect is most notable for the π bands. Hence these 3-D systems behave like simpler organic molecules, but we have the added consideration of a through-bond or hyperconjugative mixing that is specific to certain portions of k-space.

What is the thermodynamic stability of these nets relative to diamond and graphite? The calculated energy per carbon atom

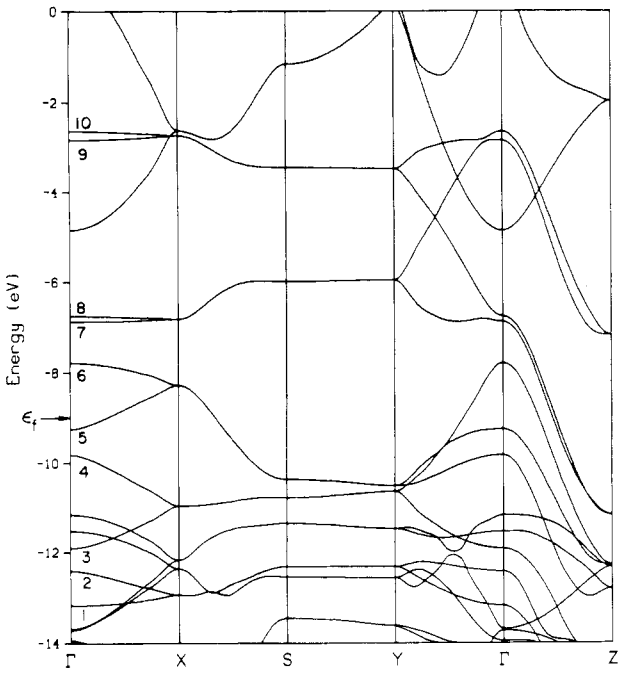

Figure 14. Calculated band structure for **11(33)**.

ordering is as follows (in eV): (**1**) 0.61, (**3**) 0.0, (**9**) 1.19, (**10**) 1.27, (**11(31)**) 0.95, (**11(32)**) 0.97, (**11(33)**) 0.86. These energies are subject to the errors associated with the EH method. As we have stated in our previous papers on this subject[1] these instabilities (relative to graphite) do not preclude the existence of these nets because the energy values (obtained by a very approximate MO method) only represent thermodynamic stability and do not take into account kinetic stability. Organic chemistry is full of examples of compounds that are thermodynamically less stable but exist anyway because of large kinetic barriers to their rearrangement. All of the nets discussed here should have large kinetic barriers for rearrangement to diamond or graphite. Many bonds have to be broken to get from one structure to another.

It is tempting to speculate that conducting 3,4-connected nets such as those advocated earlier[1] or here might be formed as local regions during the catalyzed high-pressure conversion of graphite to diamond or during the low-pressure reverse (and less rewarding) process.

Acknowledgment. Kenneth Merz thanks all of the group members for helping in familiarizing him with solid-state theory and with the programs used during the course of this research. We also acknowledge Prof. A. F. Wells for providing us with some useful comments on the derivation of nets. We also thank the Clardy group for supplying us with their version of the PLUTO program. Our research at Cornell was generously supported by the National Science Foundation through research grant DMR821722702 to the Materials Science Center. We are grateful to Jane Jorgensen and Elisabeth Fields for their expert drawings.

Appendix

The extended Hückel method[20] in the tight binding approximation[21] was used in all calculations. The parameters used for carbon and hydrogen were the following: $H_{ss} = -21.4$ eV, $H_{pp} = -11.4$ eV, $\zeta_{s,p} = 1.625$; $H_{ss} = -13.6$ eV, $\zeta_{s,p} = 1.3$, respectively. To calculate average properties for the 1-D cases a 100 point k-point set was used and for the 3-D examples a 27 point k-point set was chosen.[22]

The geometries used for the calculations are given below.

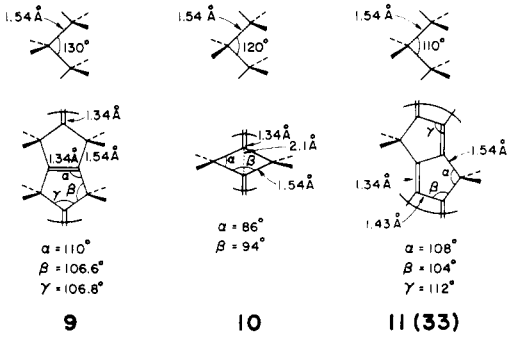

(20) Hoffmann, R. *J. Chem. Phys.* **1963**, *39*, 1397. Hoffmann, R.; Lipscomb, W. N. *J. Chem. Phys.* **1963**, *36*, 3179; **1962**, *37*, 2872.
(21) Whangbo, M.-H.; Hoffmann, R. *J. Am. Chem. Soc.* **1978**, *100*, 6093.
(22) Pack, J. D.; Monkhorst, J. H. *Phys. Rev. B* **1977**, *16*, 1748.

Design of a 4-Helix Bundle Protein: Synthesis of Peptides Which Self-Associate into a Helical Protein

Siew Peng Ho and William F. DeGrado*

Contribution from E. I. du Pont de Nemours & Company, Central Research & Development Department, Experimental Station, Building 328, Wilmington, Delaware 19898.
Received February 18, 1987

Abstract: An incremental synthetic approach is described for the design of a 4-helix bundle protein. On the basis of secondary structure prediction rules and model building, two amphiphilic 16-residue peptides, α_1A and α_1B, were designed to form α-helices that would cooperatively tetramerize (give stable 4-helix structures) in solution. The peptides were synthesized by chemical methods, and their ability to form stable helical tetramers was confirmed by molecular weight determinations and circular dichroism studies in the presence and absence of denaturant. The free energy of tetramerization of both peptides was determined to be on the order of −20 kcal/mol. In the second stage of the work, short peptidic links were inserted between the sequence of two α_1B peptides in an attempt to design a covalent cross-link between two of the helical pairs in the 4-helix bundle structure. Two peptides, α_1B-Pro-α_1B and α_1B-Pro-Arg-Arg-α_1B, were synthesized, and their tendency to form dimeric aggregates (4-helix structures) was probed. The peptide α_1B-Pro-α_1B was found to give trimeric aggregates rather than the expected dimeric structures. Incorporation of charged arginine residues in the loop achieved the desired result: the ensuing peptide, α_1B-Pro-Arg-Arg-α_1B, forms stable helical dimers in solution.

The design of large molecules with defined conformational properties is a necessary first step in the de novo design of macromolecular receptors and catalysts. To date, most of the molecules that have been designed to mimic the properties of

0002-7863/87/1509-6751$01.50/0 © 1987 American Chemical Society